Effective decoherence of realistic clocks: General theory and application to a topological insulator

Shuang Xu [1], Wei-Jiang Gong [1], H. Z. Shen [2,3] and X. X. Yi [2,3,*]

[1] College of Sciences, Northeastern University, Shenyang 110819, China

[2] Center for Quantum Sciences and School of Physics, Northeast Normal University, Changchun 130024, China

[3] Center for Advanced Optoelectronic Functional Materials Research, and Key Laboratory for UV Light-Emitting Materials and Technology of Ministry of Education, Northeast Normal University, Changchun 130024, China

(Received 22 July 2020; accepted 23 February 2021; published 5 March 2021)

It has been well established that the evolution of an isolated quantum system can appear as undergoing pure dephasing to an observer using an imperfect clock. In this work, we apply this theory to the transport phenomenon in open quantum systems. Starting with a system intrinsically undergoing nonunitary evolution in ideal time, we consider the effect of a realistic clock that approaches Gaussian distribution in the long-time limit. For quantum transport, it eventually leads to a general physical prediction: a stable probability current in a quantum transport system must be robust against any transformation that conforms with a simple formula given by an ideal Gaussian stationary clock. This understanding of quantum transport is demonstrated numerically in a topological insulator, where it also explains the robustness of the quantum Hall response against pure dephasing.

DOI: 10.1103/PhysRevA.103.032207

I. INTRODUCTION

The observation that the quantum Hall response is precisely quantized [1] led to the discovery of the topological phase of matter [2–5]. So far, it has been shown that the Hall conductivity of a topological insulator is guaranteed topologically [6,7] to be a (half) integer multiple of a constant [8], even in the presence of substrate disorder and electron-electron interaction [9,10]. Recently, there has been wide interest in topological insulators subject to external influences [11–14], such as thermalization [15–21], quantum quench [22–25], and decoherence [26–31]. In particular, it was suggested that the quantum Hall response is robust against pure dephasing [32–35]. Remarkably, both the current operator and the perturbed quantum state are shown to be nontrivially affected under pure dephasing, while the interplay between the two impacts maintains a net zero impact on the probability current [34]. This could be a mathematical coincidence, but it might also be guaranteed by an underlying general principle.

In this work, we propose a simple physical explanation for the robustness of the quantum Hall response against pure dephasing, which also gives a general principle for quantum transport under Markovian noise beyond pure dephasing. It relies on a seemingly distant concept—realistic clock.

Long ago, the difficulty of introducing a time observable [36,37] in conventional quantum theory led to the conditional probability interpretation of time, where time emerges from the entanglement between a clock subsystem and the remainder of a timeless universe [38–44]. Recently, after overcoming early criticisms [44–47], the theory received renewed interest. Since ideal time is physically inaccessible [47–49], it in turn led to the idea of relational time. That is, the time evolution of the same quantum system can be different for observers with different information of time [50]. Specifically, as simply illustrated in Fig. 1, a closed quantum system can be observed as undergoing pure dephasing without relaxation [51] to an observer using an imperfect clock [52–57].

Here, we generally start with a quantum system intrinsically obeying memoryless linear dynamics [58,59] under ideal time, and we formalize its effective dynamics as observed under a real clock. The real clock is characterized with a stochastic process of ideal time, and its behavior is generally allowed to change with clock time. When the said stochastic process has independent increments [60], a memoryless system dynamics is recovered as a series expansion fully given by the instantaneous stochastic process. Specifically, with an ideal Brownian stochastic process, we recover an effective dynamics that is formally consistent with the previous result for a Gaussian clock [53]. To overcome the causality issue of a Gaussian stationary clock, we also consider the asymptotic physical prediction of realistic clocks that approaches the ideal Gaussian stationary clock in the long-time limit, which are expected to give asymptotically identical physical predictions.

With our real clock, we eventually deliver a physical prediction in quantum transport, specifically in the Hall response of an open topological insulator [3–5]. We propose that the robustness of the Hall current against pure dephasing is guaranteed by relational time. The clock we assumed does not affect the measured value of a macroscopic stable current. Therefore, if the quantum Hall response is robust against time inaccuracy under a Gaussian stationary clock, which is in turn equivalent to pure dephasing, the quantum Hall response then has to be robust against pure dephasing, regardless of its physical cause.

Furthermore, with a generalized formula of the real clock effect, we can give more predictions on the robustness of the

*yixx@nenu.edu.cn

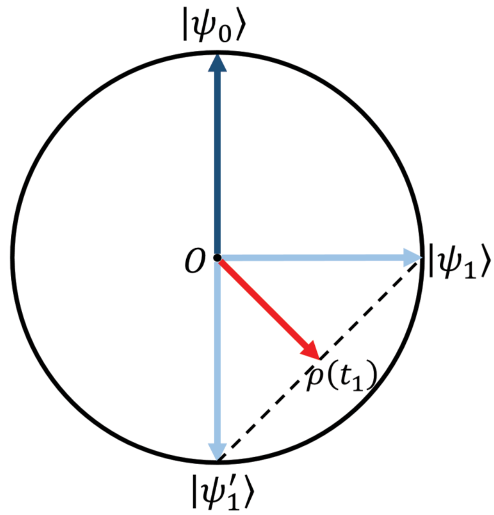

FIG. 1. A simple example of effective decoherence due to an imperfect clock. The circle is the intersection between a plane and the Bloch sphere of a closed two-level quantum system. Consider a simple extreme situation where the clock runs randomly, with equal probabilities, at one of two different rates in each repeat experiment. When the clock shows $t = 0$, the system is initialized in a pure state $|\psi_0\rangle$, but when the clock shows $t = t_1$, the system is either in $|\psi_1\rangle$ or $|\psi_1'\rangle$. The observed quantum state of the system at clock time t_1 with repeat experimentation is then $\rho(t_1) = \frac{1}{2}|\psi_1\rangle\langle\psi_1| + \frac{1}{2}|\psi_1'\rangle\langle\psi_1'|$, which is a mixed state.

Hall response. That is, a stable current in a quantum transport system must remain unchanged under transformations of its master equation that are formally identical to the real clock effect. This prediction is demonstrated numerically with the Hall conductivity of open topological insulators. It is also possible to test this prediction experimentally, most likely with a platform of ultracold atoms on an optical lattice [61–69].

The remainder of this paper is structured as follows: In Sec. II, we formalize the real clock effect for a quantum system intrinsically obeying general time-independent linear dynamics. In Sec. III, we recover the Gaussian clock and address its causality issue via the asymptotic long-time limit, and we show how specifically a Markovian master equation transforms into another time-local master equation under a Gaussian stationary clock. In Sec. IV, we show how a stable current in a quantum transport system must remain unchanged under a real clock, and we demonstrate numerically that the Hall conductivity of a two-dimensional two-band open topological insulator remains unchanged when the model is transformed according to the formula of an ideal Gaussian stationary clock. Finally, in Sec. V, we conclude and summarize our results.

II. GENERAL FORMALISM

Consider an evolving quantum system that obeys general time-independent linear dynamics in relation to ideal time. We examine how its dynamics appears in measurement under a real clock.

Similar to the work of Egusquiza [52], we characterize a real clock statistically. Specifically, we assume that the time shown by the clock (clock time) in each instance of repeat experiments is progressing on one of an infinite amount of possible paths $\gamma_i(t)$. That is, for a clock on a particular path $\gamma_i(t)$, when the clock time is t, the ideal time is actually $\gamma_i(t)$. One can imagine that the clock is moving stochastically in a "space" of ideal time as the clock time passes.

Each $\gamma_i(t)$ may or may not be a continuous function, but we assume it is continuous in probability. That is, sometimes the clock may be stuck for a finite period of ideal time, leading to a jump in trajectory $\gamma_i(t)$, but this does not happen with a finite probability during any given infinitesimal period of clock time. This stochastic continuity [70] ensures a continuous probability distribution of $\gamma_i(t)$.

Each hypothetical experiment begins with a joined measurement on the system and the clock, as a result, for every path, $\gamma_i(0) \equiv 0$. The probability for the clock to follow a particular path $\gamma_i(t)$ is denoted p_i, which satisfies $\sum_i p_i = 1$. Moreover, the clock paths are required to obey the following statistical characterizations:

$$\sum_i p_i \gamma_i(t) = t, \tag{1}$$

$$\sum_i p_i \gamma_i^2(t) = s(t) + t^2, \tag{2}$$

where it can be shown that $s(t) = \sum_i p_i[\gamma_i(t) - t]^2$, which is the variance of the ideal time at a given clock time, characterizing the level of inaccuracy.

The density matrix of the system at any given ideal time x is denoted as $\rho_S(x)$, and repeat measurements are carried out at a given clock time t. When the timing of such measurements is inconsistent, the quantum state measured at any given clock time is actually an incoherent superposition of states from different moments of the system's evolution [53]. As far as the observer is concerned, at clock time T, the system's density matrix reads

$$\rho(t) \equiv \sum_i p_i \rho_S[\gamma_i(t)]. \tag{3}$$

The change in the measurement result of the quantum state can in turn cause deviation in the observed motion trajectory, which may eventually lead to an entirely different system dynamics being extrapolated. To find the time differential formula of the observed system motion $\rho(t)$, we first generally characterize the system dynamics in ideal time as follows:

$$\frac{\partial \rho_S(x)}{\partial x} = \mathcal{M}(\rho_S[x]), \tag{4}$$

where time-independent superoperator $\mathcal{M}$ is an arbitrary linear superoperator. It generally represents a system with linear memoryless dynamics, which can be a closed quantum system, a Markovian open system, or a non-Hermitian system.

We can then apply Taylor expansion to the evolution of observed system density matrix $\rho(t)$ during an infinitesimal period of clock time between t and $t+\delta t$ as follows:

$$\begin{aligned}\rho(t+\delta t) &= \sum_i p_i \rho_S[\gamma_i(t+\delta t)] \\ &= \sum_i p_i \Big\{ \rho_S[\gamma_i(t)] + [\gamma_i(t+\delta t) - \gamma_i(t)]\dot{\rho}_S[\gamma_i(t)] \\ &\quad + \frac{1}{2}[\gamma_i(t+\delta t) - \gamma_i(t)]^2 \ddot{\rho}_S[\gamma_i(t)] + \cdots \Big\}. \end{aligned} \tag{5}$$

To recover a memoryless observed system dynamics, we have to impose another assumption: around a given clock time t, there is a lack of correlation between $[\gamma_i(t+\delta t)-\gamma_i(t)]$ and $\gamma_i(t)$. In other words, we assume that $\gamma_i(t)$, which may or may not be a continuous function, is undergoing a stochastic process with independent increments [60], which means

$$\sum_i p_i f[\gamma_i(t+\delta t)-\gamma_i(t)]g[\gamma_i(t)] = \left\{\sum_i p_i f[\gamma_i(t+\delta t)-\gamma_i(t)]\right\}\left\{\sum_j p_j g[\gamma_j(t)]\right\}, \quad (6)$$

where f and g are arbitrary functions of ideal time $\gamma_i(t)$, such as $\rho_S[\gamma_i(t)]$. Although $\gamma_i(t)$ is definitely correlated with clock time t, Eq. (6) is limited to one clock time t, and hence, at a different clock time t', $[\gamma_i(t'+\delta t)-\gamma_i(t')]$ is allowed to have a different distribution. If we also require the same distribution at all clock times, $\gamma_i(t)$ would then have to be a Lévy process [60]. We note that we do not assume the clock to always obey Eq. (6); $\gamma_i(t)$ may also violate Eq. (6) around t', in which case the subsequent result simply will not apply around t'.

Given Eq. (6) and considering that $\mathcal{M}$ is linear, Eq. (5) can be rewritten as a memoryless equation of motion as follows:

$$\dot{\rho}(t) = \mathcal{M}[\rho(t)] + \sum_{n=2}^{\infty}\frac{R_n(t)}{n!}\mathcal{M}^n[\rho(t)], \quad (7)$$

$$R_n(t) \equiv \lim_{\delta t\to 0}\frac{1}{\delta t}\sum_i p_i[\gamma_i(t+\delta t)-\gamma_i(t)]^n = \frac{\partial}{\partial\tau}\int_{-\infty}^{+\infty}x^n D_t(x;\tau)dx\bigg|_{\tau=0}, \quad (8)$$

where we denote $x(\tau)$ characterized by distribution $D_t(x;\tau)$ as a Lévy process [60] that is obeyed instantaneously by the real clock at clock time t. The distribution of $[\gamma_i(t+\delta t)-\gamma_i(t)]$ is therefore $D(\delta t, x)$, whereas $D(0,x)=\delta(x)$. According to Itô's Lemma [71,72], $\sum_i p_i[\gamma_i(t+\delta t)-\gamma_i(t)]^2$ is of $O(\delta t)$ order. We therefore give

$$\sum_i \frac{p_i}{2}[\gamma_i(t+\delta t)-\gamma_i(t)]^2 = \sum_i\frac{p_i}{2}\left\{\left[\gamma_i^2(t+\delta t)-\gamma_i^2(t)\right]-2[\gamma_i(t+\delta t)-\gamma_i(t)]\gamma_i(t)\right\}$$
$$= \frac{1}{2}[s(t+\delta t)-s(t)]+\frac{1}{2}[(t+\delta t)^2-t^2]-\sum_i p_i[\gamma_i(t+\delta t)-\gamma_i(t)]\gamma_i(t), \quad (9)$$

in which Eq. (6) gives the value of the last term above as $t\delta t$. We thereby have $R_2(t)=\dot{s}(t)$, which is guaranteed by independent increments of $\gamma_i(t)$ around clock time t, regardless of its distribution or past behavior.

III. GAUSSIAN CLOCK

A. Brownian stochastic process

To recover a particular result for our purpose, we particularly consider

$$D_t(x;\tau) = \frac{1}{\sqrt{2\pi K(t)\tau}}e^{-\frac{(x-\tau)^2}{2K(t)\tau}}, \quad (10)$$

which conforms with the Brownian stochastic process. Itô's Lemma has already given the exact value of each R_n, but it can also be found easily using Eq. (8). Either way, the result is $R_2(t)=K(t)$, while for $n>2,\ R_n(t)\equiv 0$. We then have

$$R_2(t)=K(t)=\dot{s}(t). \quad (11)$$

We thereby recover a very simple effective dynamics that conforms with all previous results [52–57],

$$\dot{\rho}(t)=\mathcal{M}[\rho(t)]+\frac{\dot{s}(t)}{2}\mathcal{M}^2[\rho(t)], \quad (12)$$

which applies around clock time t as long as the clock is undergoing an ideal Brownian stochastic process around time t. This particular class of real clock directly corresponds to pure dephasing within a unitary $\mathcal{M}$.

B. Causality issue

Apparently, according to Eq. (12), if the clock maintains a Brownian stochastic process, and $\dot{s}(t)$ remains a constant X, then the effective system observed under such a real clock will be indistinguishable from an actual system, with the time-independent dynamics given as follows:

$$\dot{\rho}=\mathcal{M}(\rho)+\frac{X}{2}\mathcal{M}^2(\rho). \quad (13)$$

We note that Egusquiza [53] has already eliminated the possibility of any clock other than an ideal Gaussian stationary clock to maintain this exact observed dynamics above.

However, an ideal Gaussian distribution only converges perfectly as $|\gamma_i(t)-t|\to\infty$. Therefore, a realistic clock cannot be in a perfect Gaussian distribution for finite time t. Moreover, as pointed out by Egusquiza [53] and can be seen from Fig. 2, this leads to a significant causality issue near $t=0$: the prediction of a Gaussian stationary clock demands that the second measurements can happen before the first, and they must contribute results according to a negative time extension of $\rho_S(x)$, which would be nonphysical, especially if $\rho_S(x)$ itself obeys dissipative dynamics.

On the other hand, as can be seen from Eq. (3), the measurement result at clock time T is determined by the distribution of $\gamma_i(T)$, and it is completely unaffected by the value of $\gamma_i(t)$ during $0<t<T$. Therefore, we generally consider an asymptotic clock that in the limit of $t\gg 0$, approaches the Gaussian distribution and also satisfies

$$s(t)\to Xt. \quad (14)$$

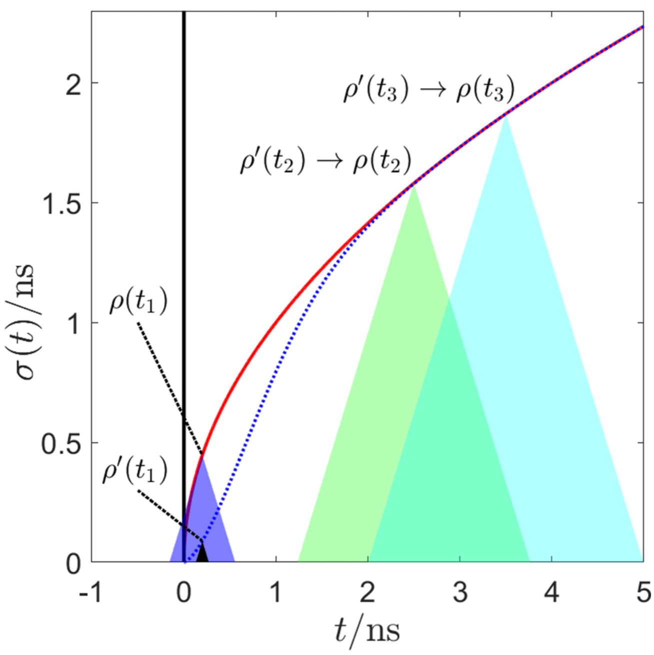

FIG. 2. An illustrative comparison of two real clocks. The red solid curve is the standard deviation $\sigma(t) = \sqrt{s(t)}$ for an ideal Gaussian stationary clock given by $s(t) = t$ ns vs clock time t, while the blue dotted curve is that of an arbitrary Gaussian clock given by $s(t) = t\ [1 - \exp(-t^2/\mathrm{ns}^2)]$ ns. Imagine a quantum system is evolving on the horizontal axis according to ideal time $x = t$; then the triangles represent Eq. (3).

As illustrated in Fig. 2, as long as all measurements are made in the long-time limit, the observer should find asymptotically no evidence that the system ever deviated from the dynamics given by the Gaussian stationary clock.

Actual physical clocks usually only track discrete intervals of time, so they might not be able to resolve time near $t = 0$. Considering that the one-dimensional random walk [73–75] is known to approach a Gaussian distribution in the limit of infinite steps, they might also satisfy Eq. (14). Regardless, an experimental framework where the model of a Gaussian stationary clock gives arbitrarily good predictions is possible. As long as this is the case, experimentally verifiable physical predictions can be extracted under a Gaussian stationary clock.

C. Master equation

Here, we specifically give how a time-independent Markovian open quantum system is transformed under a Gaussian stationary clock. Consider a general master equation,

$$\mathcal{M}(\rho) = \mathcal{H}(\rho, H) + \sum_j \mathcal{L}(\rho, V_j), \tag{15}$$

$$\mathcal{H}(\rho, H) \equiv -i[H, \rho], \tag{16}$$

$$\mathcal{L}(\rho, V_j) \equiv V_j \rho V_j^\dagger - \frac{1}{2} V_j^\dagger V_j \rho - \frac{1}{2} \rho V_j^\dagger V_j, \tag{17}$$

where H, V_j are the Hamiltonian and Lindbladians, respectively, of a Markovian open quantum system with respect to ideal time. Hence, the extra term from the effective dynamic formula reads

$$\mathcal{M}[\mathcal{M}(\rho)] = \mathcal{H}[\mathcal{H}(\rho, H), H] + \sum_{jk} \mathcal{L}[\mathcal{L}(\rho, V_j), V_k] + \sum_j \{\mathcal{L}[\mathcal{H}(\rho, H), V_j] + \mathcal{H}[\mathcal{L}(\rho, V_j), H]\}. \tag{18}$$

To further expand the expression, we find it very helpful to use the following formula:

$$2[a\rho b^\dagger + b\rho a^\dagger] = \mathcal{L}(\rho, a+b) - \mathcal{L}(\rho, a-b) + \{\rho, a^\dagger b + b^\dagger a\}, \tag{19}$$

where a, b are arbitrary linear operators. Tedious but straightforward derivation then gives

$$\mathcal{H}[\mathcal{H}(\rho, H), H] = 2\mathcal{L}(\rho, H); \tag{20}$$

$$\mathcal{L}[\mathcal{H}(\rho, H), V_j] + \mathcal{H}[\mathcal{L}(\rho, V_j), H] = \tfrac{1}{2}[-\mathcal{H}(\rho, \{V_j^\dagger V_j, H\}) + \mathcal{X}(\rho, V_j, \{V_j, -iH\}) + \mathcal{X}(\rho, iH, V_j^\dagger V_j)]; \tag{21}$$

$$\mathcal{L}[\mathcal{L}(\rho, V_j), V_k] = \mathcal{L}(\rho, V_k V_j) - \tfrac{1}{4}[\mathcal{X}(\rho, V_k V_j^\dagger V_j, V_k) + \mathcal{X}(\rho, V_k^\dagger V_k V_j, V_j)] + \tfrac{1}{8}[\mathcal{X}(\rho, V_j^\dagger V_j, V_k^\dagger V_k) + \mathcal{H}(\rho, i[V_k^\dagger V_k, V_j^\dagger V_j])], \tag{22}$$

where we denote

$$\mathcal{X}(\rho, V_j, V_k) \equiv \mathcal{L}(\rho, V_j + V_k) - \mathcal{L}(\rho, V_j - V_k), \tag{23}$$

which satisfies

$$\mathcal{X}(\rho, V_j, V_k) = \mathcal{X}(\rho, V_k, V_j) = -\mathcal{X}(\rho, V_j, -V_k). \tag{24}$$

Note that $i[V_k^\dagger V_k, V_j^\dagger V_j]$ can be shown as Hermitian.

Apparently, a system obeying a Markovian master equation under ideal time can appear as obeying a different master equation under an ideal Gaussian stationary clock, or the corresponding asymptotic clock if only measured in the long-time limit. Here, this new effective master equation is fully expressed with a correction to the Hamiltonian as well as a series of additional Lindbladians.

We note that there is an issue here for an ideal stationary Gaussian clock due to causality violation. Equation (3) naturally guarantees the linear dynamical map to satisfy completely positive and trace preserving [76] for any positively defined ideal time distribution. However, an ideal Gaussian stationary clock may not follow the same rule near $t = 0$ due to the nontrivial weight of the negative time extension of $\rho_S(x)$, as shown in Fig. 2. In some special cases, the result of Eq. (13) might not be physical, which explains why the decay rates of some of the Lindbladians are negative in the general formalism above.

IV. ROBUSTNESS OF QUANTUM HALL RESPONSE

When the effect of an imperfect clock and the effect of an environment could both cause the same changes in the observed evolution of a quantum system, one would not be able to distinguish the two just by observing the system in question. Since the mechanism of the real clock effect governs both macroscopic measurement and quantum state evolution, this indistinguishability can be used to deliver physical predictions. Particularly, for a stable probability current in an open system, the fact that no change is expected to happen under a real clock can be generalized to a class of master equations realized by mechanisms other than the real clock.

A. Robustness of current under real clock effect

In order to show that the measured mean value of a stable current carried by a quantum transport system during the time interval between t_1 and t_2 remains unaltered under an asymptotic real clock satisfying Eq. (14) in the limit of $t_1, t_2 \gg 0$, consider a general scenario as follows: a quantum system with a stable electric current J_0 transports electrons from one reservoir to another.

In ideal time, to obtain the current of a transport system, one repeatedly observes the number of electrons in the destination reservoir for two different moments, respectively. We note that the measurement is only carried out at one of the moments in each iteration of the experiment. If the probability current of each electron is a stable value J_0 during the range of time when electron numbers are measured, and if the probability of finding $N_j(t)$ electrons at time t is denoted q_j, we have

$$\sum_j q_j N_j(t) = J_0 t + N_0, \tag{25}$$

$$J_0 = \frac{1}{t_2 - t_1}\left[\sum_j q_j N_j(t_2) - \sum_j q_j N_j(t_1)\right], \tag{26}$$

where N_0 is a constant number.

In a repeat measurement under a real clock, however, both the actual measurement time $\gamma_i(t)$ and the population of electrons $N_j(t)$ fluctuate statistically in different iterations. Nevertheless, considering that there is no correlation between p_i and q_j, the measured stable current in this case can still be expressed as

$$\bar{J} = \frac{1}{t_2 - t_1}\sum_{ij} p_i q_j \{N_j[\gamma_i(t_2)] - N_j[\gamma_i(t_1)]\}. \tag{27}$$

Given Eq. (1), it can then be shown that $\bar{J} = J_0$.

Note that as long as the hypothetical clock is valid, we are not required to physically have such a clock to utilize relational time any more than we would need a moving object to change the frame of reference. Given an ideal system obeying Eq. (4) that produces a stable current J_0, with or without actually having the clock, we know, in the corresponding relational time, that it would effectively obey Eq. (13) and produce $\bar{J}$. It can then be reasoned that any system undergoing the same dynamics as Eq. (13) must also produce $\bar{J}$ because it obeys the same dynamics that we know produces $\bar{J}$, which in turn equals J_0.

In other words, for a class of quantum systems with master equations in the form of Eq. (13) with the same superoperator $\mathcal{M}$ and different non-negative number X, if they are all carrying stable currents, the magnitude of their currents should all be equal, regardless of the mechanism realizing their master equations.

B. Model

Specifically, we examine the case of a topological insulator, where a stable current response in the y direction occurs under a weak electric field in the x direction. The linearized relation between the current density and the electric field is characterized by Hall conductivity. In each momentum-conserving subspace of its Hilbert space, the master equation of a general open topological insulator is given by

$$\mathcal{M}_k(\rho_k) = \mathcal{H}[\rho_k, H(k)] + \mathcal{L}[\rho_k, \sqrt{g_{\mathrm{D}}}H(k)] + \mathcal{L}[\rho_k, \sqrt{g_{\mathrm{SLD}}}\sigma_z] + \mathcal{L}[\rho_k, \sqrt{g_{\mathrm{SLC}}}\sigma_-], \tag{28}$$

where index $k = (k_x, k_y)$ denotes momentum, with ρ_k being the density matrix within the momentum-conserving subspace. Also, g_{D} characterizes the rate of pure dephasing in the basis of Hamiltonian eigenstates, g_{SLD} characterizes the rate of site-local pure dephasing, and g_{SLC} characterizes the rate of site-local cooling. σ_l, where $l = x, y, z$, are Pauli matrices, and $\sigma_- = (\sigma_x - i\sigma_y)/2$.

Here, we choose a particular model of two-dimensional topological insulators, the Chern insulator, which has a Hamiltonian as follows:

$$H(k) = \{\sigma_x \sin k_x + \sigma_y \sin k_y + \sigma_z[m + \cos k_x + \cos k_y]\}\mathrm{ns}^{-1}, \tag{29}$$

where $0 \leqslant k_x, k_y < 2\pi$, and $m = -1.5$ is an arbitrary parameter that affects the topology of the topological insulator.

A very weak static electric field in the x direction is characterized by Peierls substitution,

$$k \rightarrow k - \frac{eE}{\hbar}t, \tag{30}$$

where $-e$ is the electric charge of an electron and $E \rightarrow 0$ is the magnitude of the electric field. We note that the alternative time-independent scalar potential characterization of the static electric field, albeit unsolvable, justifies the use of the real clock.

The system is initialized as $\rho_k(0) = e^{-\beta H(k)}$, where $\beta = 10\mathrm{ns}$ is used to characterize a near-zero temperature, and $H(k)$ is the original Hamiltonian of the system. This initial state remains unchanged, even if the effective Hamiltonian is altered under the real clock effect.

As the system evolves, the current contribution in the y direction can be extracted from the instantaneous density matrix within each momentum-conserving subspace. Here, we denote

$$I_y(t) = \frac{-e}{E_x}\int_{BZ} dk \mathrm{Tr}\left[\frac{\partial H(k)}{\partial k_y}\rho_k(t)\right], \tag{31}$$

$$J_y(t) = \frac{-e}{E_x}\int_{BZ} dk \mathrm{Tr}[\hat{J}_y(k)\rho_k(t)], \tag{32}$$

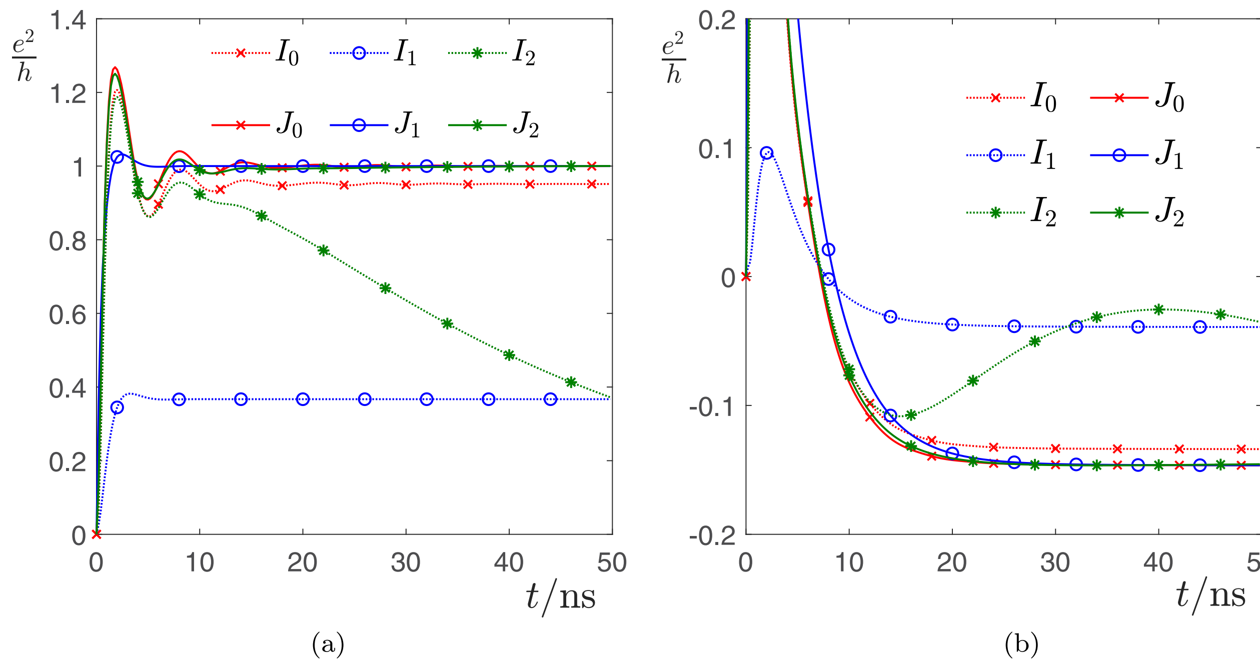

FIG. 3. Compared results of numerical simulations of Hall conductivities. The dotted lines I_0, I_1, I_2, are $I_y(t)$, with $H(k)$ being the original Hamiltonian from Eq. (29) but subject to Eq. (30). These dotted lines do not represent current, but they reflect the evolution of the tiny perturbation in the quantum state responsible for the Hall response. The solid lines J_0, J_1, J_2, are $J_y(t)$, with $\hat{J}_y(t)$ given by the complete (effective) master equation. These solid lines give the actual Hall conductivity in their respective situation. I_0, J_0 are given for the original system, I_1, J_1 are given under Eq. (34), and I_2, J_2 are given under Eq. (35). The two figures are given using different parameters: (a) $g_{\mathrm{HD}} = 0.25\mathrm{ns}^{-1}$, $g_{\mathrm{SLD}} = g_{\mathrm{SLC}} = 0$; (b) $g_{\mathrm{HD}} = 0.25\mathrm{ns}^{-1}$, $g_{\mathrm{SLD}} = 0.09\mathrm{ns}^{-1}$, $g_{\mathrm{SLC}} = 0.25\mathrm{ns}^{-1}$.

where $I_y(t)$ is given by the current operator for the closed translationally invariant tight-binding model, which we employ to reveal the density matrix evolution. However, the current operator can be different in open systems [77], so the value of $I_y(t)$ is not the actual Hall conductivity unless the system is closed. The actual Hall conductivity $J_y(t)$ must be given by the current operator for Markovian open tight-binding systems [35], in which

$$\hat{J}_y(k) = \frac{\partial H(k)}{\partial k_y} + \sum_j \frac{i\gamma_j}{2}\left[\frac{\partial V_{k,j}^\dagger}{\partial k_y}V_{k,j} - V_{k,j}^\dagger\frac{\partial V_{k,j}}{\partial k_y}\right], \quad (33)$$

where $V_{k,j}^\dagger$ are all of the Lindbladians in the master equation for $\rho_k(t)$. Note that the second term is 0 if the system is closed, and Eqs. (20)–(22) are sufficiently expanded for a numerical implementation of this operator. The coefficient $\gamma_j \equiv 1$, since this value is instead incorporated into $V_{k,j}^\dagger$. Note that the formula of an open-system current operator also changes as the master equation itself is transformed.

C. Numerical results

We do not have a general formula for the open-system Hall response of a topological insulator; the demonstration for the generalized situation is therefore numerical.

On top of the system dynamics $\mathcal{M}$ given in Eqs. (28) and (29), two different settings for Eq. (13) are considered, which are characterized as follows:

$$X = 1\mathrm{ns}, \quad (34)$$

$$X'(t) = \frac{t}{T}\mathrm{ns}, \quad (35)$$

where T is the full simulation time. With Eq. (34), the constant-rate increase of variance is consistent with the one-dimensional random walk; and with Eq. (35), the effective master equations slowly move within the current conserving class given by Eq. (13).

As shown in Fig. 3, two different original systems are simulated with their respective parameters based on Eq. (28). As shown in their respective figures, for each original system, two transformed systems are also simulated. Their master equations are given by Eq. (13) with the two settings characterized above.

In each figure, the values of I_0, I_1, I_2 are means of the same observable on density matrices from the original system and the two transformed systems. However, in each figure, these values are not identical. Apparently, the original system and different transformed systems given by X and $X'(t)$ can be in different quantum states. The values of I_2 in each figure are changing with $X'(t)$ throughout the simulation. This clearly shows that the change in parameter $X'(t)$ is nontrivial to the perturbation of the quantum state.

Moreover, since I_0, I_1, I_2 are given by the same operators at any given time, it shows that the linear response of the electrons' quantum state is different under different settings corresponding to different clocks. Without also considering the corresponding changes in the current observable, these changes are not trivial in terms of the electric current contribution.

However, J_0, J_1, J_2, which are given by open-system current operators that also change with the value of parameter X from Eq. (13), eventually stabilize at the same value in each figure. As predicted, the actual electric currents in the transformed systems are identical to that in the original system. In particular, as the second transformed system slowly moves within the current-conserving class given by Eq. (13), the Hall conductivity also stabilizes at the original value and remains unchanged.

Finally, we note that an experimental test of this prediction is also possible. The simplest experiment requires the engineering of two topological insulators obeying different master equations from the same class as defined in Eq. (13). To implement such systems, instead of actual solid-state matter, one may rely on the highly flexible [69] quantum simulation platform of ultracold atoms on an optical lattice. For nontrivial results, it is preferred that both of them are carrying currents that are no longer quantized under environmental influence (similar to the simulation of Fig. 3). If the measured Hall conductivities were identical, then the prediction "survived."

V. DISCUSSION AND CONCLUSION

In conclusion, we give an explanation for the robustness of the quantum Hall response against pure dephasing based on the theory of the real clock. We also generalized the theory of the real clock to systems that are intrinsically nonunitary under ideal time, which then gives experimentally verifiable predictions for quantum transport in open quantum systems.

Starting with a quantum system obeying arbitrary linear memoryless dynamics that may or may not be unitary, we formalized its corresponding effective system to an observer using a real clock. We show that whenever the clock is undergoing a stochastic process with independent increments, the effective system will obey another memoryless dynamics given by Eq. (7). Specifically, for an ideal Gaussian stationary clock, we give the effective master equation of the observed system. As expected, it is a series of Lindbladian terms on top of a corrected Hamiltonian. However, in this most general formalism, some of the Lindbladian terms are with negative decay rate.

Due to the causality issue, it is not realistic to expect a physical clock in real life to satisfy the ideal Brownian stochastic process. To overcome this issue, we consider instead a hypothetical clock that approaches the same ideal time distribution of a Gaussian stochastic clock in the long-time limit. In this context, the physical predictions of a Gaussian stationary clock can still be considered as asymptotically accurate.

For two quantum systems carrying stable currents, we show that as long as their master equations can be transformed into one another via the given formula of Eq. (13), the stable currents carried by these two systems must be equal. This prediction is demonstrated numerically in a model of the open-system quantum Hall effect, and we note that the same principle holds even when the two systems are realized by effects other than the real clock.

ACKNOWLEDGMENTS

This work is supported by the National Natural Science Foundation of China (NSFC) under Grants No. 11775048 and No. 12047566, Fundamental Research Funds for the Central Universities (Grants No. N2005022, No. N2002005, and No. 2412019FZ044), the LiaoNing Revitalization Talents Program (Grant No. XLYC1907033), and the Liaoning BaiQianWan Talents Program (Grant No. 201892126).

[1] K. V. Klitzing, G. Dorda, and M. Pepper, New Method for High-Accuracy Determination of the Fine-Structure Constant Based on Quantized Hall Resistance, Phys. Rev. Lett. **45**, 494 (1980).
[2] F. D. M. Haldane, Model for a Quantum Hall Effect without Landau Levels: Condensed-Matter Realization of the "Parity Anomaly," Phys. Rev. Lett. **61**, 2015 (1988).
[3] J. E. Moore, The birth of topological insulators, Nature (London) **464**, 194 (2010).
[4] M. Z. Hasan and C. L. Kane, Colloquium: Topological insulators, Rev. Mod. Phys. **82**, 3045 (2010).
[5] X.-L. Qi and S.-C. Zhang, Topological insulators and superconductors, Rev. Mod. Phys. **83**, 1057 (2011).
[6] B. A. Bernevig and T. L. Hughes, *Topological Insulators and Topological Superconductors* (Princeton University Press, Princeton, NJ, 2013).
[7] N. R. Cooper, J. Dalibard, and I. B. Spielman, Topological bands for ultracold atoms, Rev. Mod. Phys. **91**, 015005 (2019).
[8] L. Zhang, Y. Zhang, J. Camacho, M. Khodas, and I. Zaliznyak, The experimental observation of quantum Hall effect of $l = 3$ chiral quasiparticles in trilayer graphene, Nat. Phys. **7**, 953 (2011).
[9] Q. Niu and D. J. Thouless, Quantized adiabatic charge transport in the presence of substrate disorder and many-body interaction, J. Phys. A: Math. Gen. **17**, 2453 (1984).
[10] S. Michalakis, Why is the Hall conductance quantized? Nat. Rev. Phys. **2**, 392 (2020).
[11] S. Vajna, B. Horovitz, B. Dóra, and G. Zaránd, Floquet topological phases coupled to environments and the induced photocurrent, Phys. Rev. B **94**, 115145 (2016).
[12] Á. Rivas and M. A. Martin-Delgado, Topological Heat Transport and Symmetry-Protected Boson Currents, Sci. Rep. **7**, 6350 (2017).
[13] T. Yoshida, K. Kudo, H. Katsura, and Y. Hatsugai, Fate of fractional quantum Hall states in open quantum systems: Characterization of correlated topological states for the full Liouvillian, Phys. Rev. Res. **2**, 033428 (2020).
[14] Y. W. Huang, P. Y. Yang, and W. M. Zhang, Quantum theory of dissipative topological systems, Phys. Rev. B **102**, 165116 (2020).
[15] K. S. Novoselov, Z. Jiang, Y. Zhang, S. V. Morozov, H. L. Stormer, U. Zeitler, J. C. Maan, G. S. Boebinger, P. Kim, and A. K. Geim, Room-temperature quantum Hall effect in graphene, Science **315**, 1379 (2007).

[16] A. Rivas, O. Viyuela, and M. A. Martin-Delgado, Density-matrix Chern insulators: Finite-temperature generalization of topological insulators, Phys. Rev. B **88**, 155141 (2013).
[17] O. Viyuela, A. Rivas, and M. A. Martin-Delgado, Uhlmann Phase as a Topological Measure for One-Dimensional Fermion Systems, Phys. Rev. Lett. **112**, 130401 (2014).
[18] O. Viyuela, A. Rivas, and M. A. Martin-Delgado, Two-Dimensional Density-Matrix Topological Fermionic Phases: Topological Uhlmann Numbers, Phys. Rev. Lett. **113**, 076408 (2014).
[19] O. Viyuela, A. Rivas, and M. A. Martin-Delgado, Symmetry-protected topological phases at finite temperature, 2D Mater. **2**, 034006 (2015).
[20] O. Viyuela, A. Rivas, S. Gasparinetti, A. Wallraff, S. Filipp, and M. A. Martin-Delgado, Observation of topological Uhlmann phases with superconducting qubits, npj Quantum Inf. **4**, 10 (2018).
[21] R. Arouca, S. N. Kempkes, and C. Morais Smith, Thermodynamics of a higher-order topological insulator, Phys. Rev. Res. **2**, 023097 (2020).
[22] M. D. Caio, N. R. Cooper, and M. J. Bhaseen, Quantum Quenches in Chern Insulators, Phys. Rev. Lett. **115**, 236403 (2015).
[23] P. Wang, M. Schmitt, and S. Kehrein, Universal nonanalytic behavior of the Hall conductance in a Chern insulator at the topologically driven nonequilibrium phase transition, Phys. Rev. B **93**, 085134 (2016).
[24] M. D. Caio, N. R. Cooper, and M. J. Bhaseen, Hall response and edge current dynamics in Chern insulators out of equilibrium, Phys. Rev. B **94**, 155104 (2016).
[25] J. H. Wilson, J. C. Song, and G. Refael, Remnant Geometric Hall Response in a Quantum Quench, Phys. Rev. Lett. **117**, 235302 (2016).
[26] Y. Xing, Q.-F. Sun, and J. Wang, Influence of dephasing on the quantum Hall effect and the spin Hall effect, Phys. Rev. B **77**, 115346 (2008).
[27] J.-C. Chen, H. Zhang, S.-Q. Shen, and Q.-F. Sun, Dephasing effect on transport of a graphene p-n junction in a quantum Hall regime, J. Phys.: Condens. Matter **23**, 495301 (2011).
[28] J. E. Avron, M. Fraas, G. M. Graf, and O. Kenneth, Quantum response of dephasing open systems, New J. Phys. **13**, 053042 (2011).
[29] H. Z. Shen, W. Wang, and X. X. Yi, Hall conductance and topological invariant for open systems, Sci. Rep. **4**, 6455 (2014).
[30] H. Z. Shen, M. Qin, X. Q. Shao, and X. X. Yi, General response formula and application to topological insulator in quantum open system, Phys. Rev. E **92**, 052122 (2015).
[31] H. Z. Shen, H. Li, Y. F. Peng, and X. X. Yi, Mechanism for Hall conductance of two-band systems against decoherence, Phys. Rev. E **95**, 042129 (2017).
[32] H. Jiang, S. Cheng, Q.-F. Sun, and X. C. Xie, Topological Insulator: A New Quantized Spin Hall Resistance Robust to Dephasing, Phys. Rev. Lett. **103**, 036803 (2009).
[33] J. E. Avron, M. Fraas, and G. M. Graf, Adiabatic response for Lindblad dynamics, J. Stat. Phys. **148**, 800 (2012).
[34] V. V. Albert, B. Bradlyn, M. Fraas, and L. Jiang, Geometry and Response of Lindbladians, Phys. Rev. X **6**, 041031 (2016).
[35] S. Xu, H. Z. Shen, and X. X. Yi, Current in an open tight-binding system, Phys. Rev. A **99**, 012102 (2019).
[36] A. Peres, Measurement of time by quantum clocks, Am. J. Phys. **48**, 552 (1980).
[37] L. Loveridge and T. Miyadera, Relative quantum time, Found. Phys. **49**, 549 (2019).
[38] D. N. Page and W. K. Wootters, Evolution without evolution: Dynamics described by stationary observables, Phys. Rev. D **27**, 2885 (1983).
[39] E. Moreva, G. Brida, M. Gramegna, V. Giovannetti, L. Maccone, and M. Genovese, Time from quantum entanglement: An experimental illustration, Phys. Rev. A **89**, 052122 (2014).
[40] E. Moreva, M. Gramegna, G. Brida, L. Maccone, and M. Genovese, Quantum time: Experimental multitime correlations, Phys. Rev. D **96**, 102005 (2017).
[41] K. L. H. Bryan and A. J. M. Medved, Realistic clocks for a universe without time, Found. Phys. **48**, 48 (2018).
[42] A. Nikolova, G. K. Brennen, T. J. Osborne, G. J. Milburn, and T. M. Stace, Relational time in anyonic systems, Phys. Rev. A **97**, 030101(R) (2018).
[43] A. R. H. Smith and M. Ahmadi, Quantizing time: Interacting clocks and systems, Quantum **3**, 160 (2019).
[44] L. R. S. Mendes and D. O. Soares-Pinto, Time as a consequence of internal coherence, Proc. R. Soc. A **475**, 20190470 (2019).
[45] R. Gambini, R. A. Porto, J. Pullin, and S. Torterolo, Conditional probabilities with Dirac observables and the problem of time in quantum gravity, Phys. Rev. D **79**, 041501(R) (2009).
[46] V. Giovannetti, S. Lloyd, and L. Maccone, Quantum time, Phys. Rev. D **92**, 045033 (2015).
[47] C. Marletto and V. Vedral, Evolution without evolution and without ambiguities, Phys. Rev. D **95**, 043510 (2017).
[48] V. Bužek, R. Derka, and S. Massar, Optimal Quantum Clocks, Phys. Rev. Lett. **82**, 2207 (1999).
[49] M. Mullan and E. Knill, Optimizing passive quantum clocks, Phys. Rev. A **90**, 042310 (2014).
[50] R. Peierls, In defense of measurement, Phys. World **4**, 19 (1991).
[51] C. Benedetti and M. G. A. Paris, Effective dephasing for a qubit interacting with a transverse classical field, Intl. J. Quantum Inf. **12**, 1461004 (2014).
[52] I. L. Egusquiza, L. J. Garay, and J. M. Raya, Quantum evolution according to real clocks, Phys. Rev. A **59**, 3236 (1999).
[53] I. L. Egusquiza and L. J. Garay, Real clocks and the Zeno effect, Phys. Rev. A **68**, 022104 (2003).
[54] R. Gambini, R. A. Porto, and J. Pullin, A relational solution to the problem of time in quantum mechanics and quantum gravity: A fundamental mechanism for quantum decoherence, New J. Phys. **6**, 45 (2004).
[55] R. Gambini, R. A. Porto, and J. Pullin, Realistic Clocks, Universal Decoherence, and the Black Hole Information Paradox, Phys. Rev. Lett. **93**, 240401 (2004).
[56] R. Gambini and J. Pullin, Relational physics with real rods and clocks and the measurement problem of quantum mechanics, Found. Phys. **37**, 1074 (2007).
[57] V. Corbin and N. J. Cornish, Semi-classical limit and minimum decoherence in the conditional probability interpretation of quantum mechanics, Found. Phys. **39**, 474 (2009).
[58] C. Gardiner and P. Zoller, *Quantum Noise* (Springer-Verlag, Berlin, 2004).
[59] H.-P. Breuer and F. Petruccione, *The Theory of Open Quantum Systems* (Oxford University Press, Oxford, 2007).

[60] O. Kallenberg, *Random Measures, Theory and Applications, Vol. 77 of Probability Theory and Stochastic Modelling* (Springer International, Cham, 2017).

[61] M. Lewenstein, A. Sanpera, V. Ahufinger, B. Damski, A. Sen(De), and U. Sen, Ultracold atomic gases in optical lattices: Mimicking condensed matter physics and beyond, Adv. Phys. **56**, 243 (2007).

[62] I. Bloch, J. Dalibard, and S. Nascimbène, Quantum simulations with ultracold quantum gases, Nat. Phys. **8**, 267 (2012).

[63] M. Aidelsburger, M. Atala, M. Lohse, J. T. Barreiro, B. Paredes, and I. Bloch, Realization of the Hofstadter Hamiltonian with Ultracold Atoms in Optical Lattices, Phys. Rev. Lett. **111**, 185301 (2013).

[64] G. Jotzu, M. Messer, R. Desbuquois, M. Lebrat, T. Uehlinger, D. Greif, and T. Esslinger, Experimental realization of the topological Haldane model with ultracold fermions, Nature (London) **515**, 237 (2014).

[65] C.-C. Chien, S. Peotta, and M. Di Ventra, Quantum transport in ultracold atoms, Nat. Phys. **11**, 998 (2015).

[66] J. C. Budich, P. Zoller, and S. Diehl, Dissipative preparation of Chern insulators, Phys. Rev. A **91**, 042117 (2015).

[67] N. Barberán, D. Dagnino, M. A. García-March, A. Trombettoni, J. Taron, and M. Lewenstein, Quantum simulation of conductivity plateaux and fractional quantum Hall effect using ultracold atoms, New J. Phys. **17**, 125009 (2015).

[68] D. W. Zhang, Y. Q. Zhu, Y. X. Zhao, H. Yan, and S. L. Zhu, Topological quantum matter with cold atoms, Adv. Phys. **67**, 253 (2018).

[69] F. Schäfer, T. Fukuhara, S. Sugawa, Y. Takasu, and Y. Takahashi, Tools for quantum simulation with ultracold atoms in optical lattices, Nat. Rev. Phys. **2**, 411 (2020).

[70] D. Applebaum, Lévy processes–From probability to finance and quantum groups, Notices Amer. Math. Soc. **51**, 1336 (2004).

[71] S. L. Adler, Weisskopf-Wigner decay theory for the energy-driven stochastic Schrödinger equation, Phys. Rev. D **67**, 025007 (2003).

[72] J. L. McCauley, *Stochastic Calculus and Differential Equations for Physics and Finance* (Cambridge University Press, Cambridge, 2013).

[73] S. Chandrasekhar, Stochastic problems in physics and astronomy, Rev. Mod. Phys. **15**, 1 (1943).

[74] G. F. Lawler and V. Limic, *Random Walk: A Modern Introduction* (Cambridge University Press, Cambridge, 2010).

[75] O. C. Ibe, *Elements of Random Walk and Diffusion Processes* (Wiley, Hoboken, NJ, 2013).

[76] M. M. Wolf, J. Eisert, T. S. Cubitt, and J. I. Cirac, Assessing Non-Markovian Quantum Dynamics, Phys. Rev. Lett. **101**, 150402 (2008).

[77] K. V. Hovhannisyan and A. Imparato, Quantum current in dissipative systems, New J. Phys. **21**, 052001 (2019).